Pre-conditioned layered electrodes for lithium batteries

J.-S. Kim, C.S. Johnson, J.T. Vaughey, M.M. Thackeray [*]

Chemical Engineering Division, Argonne National Laboratory, Argonne, IL 60439, USA

Abstract

Layered $Li(Co_{0.33}Mn_{0.33}Ni_{0.33})O_2$ and composite $0.3Li_2MnO_3 \cdot 0.7LiMn_{0.5}Ni_{0.5}O_2$ electrode powders have been treated with NH_3 and HNO_3 prior to cell assembly. These pre-conditioning reactions improve the electrochemical properties of the electrodes when charged to high electrochemical potentials (≥ 4.45 V versus Li^0) in lithium cells. NH_3-treatment of $Li(Co_{0.33}Mn_{0.33}Ni_{0.33})O_2$ increases electrode capacity and improves the coulombic efficiency of the electrochemical reaction after the first charge/discharge cycle, whereas acid-treatment of $0.3Li_2MnO_3 \cdot 0.7LiMn_{0.5}Ni_{0.5}O_2$ electrodes significantly improves the coulombic efficiency of the initial charge/discharge reaction.
© 2005 Elsevier B.V. All rights reserved.

Keywords: Lithium battery; Layered electrode; Composite electrode; Pre-condition

1. Introduction

Considerable progress has been made in recent years to improve the stability and electrochemical properties of layered $LiMO_2$ electrodes for lithium-ion cells by using a combination of manganese, nickel and cobalt in the transition metal ion (M) layers. Particular interest has been placed on compounds, such as $Li(Mn_{0.5}Ni_{0.5})O_2$ [1–4] and $Li(Co_{1-2x}Mn_xNi_x)O_2$ [5–8] in which the manganese and nickel ions are predominantly tetravalent and divalent, respectively. In such systems, the electrochemical capacity is derived predominantly from redox reactions on the nickel and cobalt ions. The relatively high concentration of inactive Mn^{4+} ions that remains constant throughout charge and discharge is believed to contribute to the enhanced stability of these types of electrodes compared to those containing only cobalt and nickel. When additional lithium is used and incorporated into M layers that contain manganese, then the compounds can be reformulated in composite notation as $xLi_2MnO_3 \cdot (1-x)LiMO_2$ [9–11]. For example, the electrode systems $Li(Co_{1-x}Li_{0.33x}Mn_{0.67x})O_2$ ($0 \leq x \leq 1$) [12] and $Li(Ni_yLi_{[0.33-0.67y]}Mn_{[0.67-0.33y]})O_2$ ($0 \leq y \leq 0.5$) [13] can be represented in composite notation as $(2x)Li_2MnO_3 \cdot 3(1-x)LiCoO_2$ and $(1-2y)Li_2MnO_3 \cdot (3y)$ $LiMn_{0.5}Ni_{0.5}O_2$ for the same ranges of x and y, respectively. The structures of these two-component systems are highly complex. Recent nuclear magnetic resonance, X-ray absorption and high-resolution transmission electron microscopy studies of composite electrodes, such as $Li_2MnO_3 \cdot LiCrO_2$ (alternatively, $Li(Li_{0.2}Mn_{0.4}Cr_{0.4})O_2$ [14,15]) and $0.3Li_2TiO_3 \cdot 0.7LiMn_{0.5}Ni_{0.5}O_2$ (alternatively, $Li(Li_{0.13}Ti_{0.26}Mn_{0.30}Ni_{0.30})O_2$ [11]) have shown that the cations are distributed non-uniformly in the M layers, giving rise to structures with Li_2MnO_3- or Li_2TiO_3-like features and short-range order.

Layered $LiMO_2$ electrodes containing nickel and cobalt in the presence of manganese are more tolerant to electrochemical cycling when charged to a potential >4.2 V (versus Li^0) compared to their $LiCo_{1-x}Ni_xO_2$ counterparts. Although considerably higher capacities can be achieved from $Li(Co_{0.33}Mn_{0.33}Ni_{0.33})O_2$ and composite $xLi_2MnO_3 \cdot (1-x)LiMO_2$ (M = Mn, Ni, Co) electrodes by charging them to 4.6 V or higher, the coulombic efficiency on the initial charge/discharge cycle can be unacceptably low (70–80%) [11,13]. For $LiMO_2$ electrodes, this poor performance has been attributed predominantly to the loss of oxygen from the electrode surface, either as a gas or by chemical reaction with the electrolyte. The loss of oxygen occurs with a concomitant reduction of the electrode surface. By

* Corresponding author. Tel.: +1 630 252 9184; fax: +1 630 252 4176.
E-mail address: thackeray@cmt.anl.gov (M.M. Thackeray).

contrast, in composite $x\text{Li}_2\text{MnO}_3 \cdot (1-x)\text{LiMO}_2$ electrodes, lithium can be extracted electrochemically from the Li_2MnO_3 ($\text{Li}_2\text{O} \cdot \text{MnO}_2$) component of the electrode above 4.2 V with the concomitant loss of oxygen, which results in a net loss of Li_2O from the electrode structure [11,13]. In this instance, the combined electrochemical/chemical processes yield an electrochemically active MnO_2 species at the surface of the composite electrode, thereby increasing its overall capacity. In this respect, it has already been reported that Li_2O can also be removed chemically from Li_2MnO_3 by acid-treatment (a process that occurs with some H^+–Li^+ ion-exchange) to yield a layered $\text{Li}_{2-2y}\text{MnO}_{3-y}$-type structure [16–18]; it has also been previously demonstrated that oxygen can be stripped from spinel structures, such as $\text{Li}(\text{Li}_{0.33}\text{Mn}_{1.67})\text{O}_4$ by ammonia reduction to yield oxygen-deficient $\text{Li}(\text{Li}_{0.33}\text{Mn}_{1.67})\text{O}_{4-\delta}$ compounds [19]. It stands to reason, therefore, that it might be possible to reduce the coulombic inefficiency of LiMO_2 and composite $x\text{Li}_2\text{MnO}_3 \cdot (1-x)\text{LiMO}_2$ electrodes during the initial charge/discharge cycle by pre-conditioning LiMO_2 electrodes with a mild reducing agent, such as ammonia (to imitate oxygen loss) and by pre-conditioning $x\text{Li}_2\text{MnO}_3 \cdot (1-x)\text{LiMO}_2$ electrodes with acid (to imitate Li_2O loss from the Li_2MnO_3 component). It was envisaged that pre-conditioning might generate the stable structural configuration that is induced electrochemically during the initial charge of these electrodes at high potentials, at least at the electrode surface. We have, therefore, used these pre-conditioning strategies in attempts to improve the stability and coulombic efficiency of $\text{Li}(\text{Co}_{0.33}\text{Mn}_{0.33}\text{Ni}_{0.33})\text{O}_2$ and composite $0.3\text{Li}_2\text{MnO}_3 \cdot 0.7\text{LiMn}_{0.5}\text{Ni}_{0.5}\text{O}_2$ electrodes when charged to voltages greater than 4.45 V in lithium cells. In this paper, we report our preliminary results of these studies.

2. Experimental

2.1. Synthesis

$\text{Li}(\text{Co}_{0.33}\text{Mn}_{0.33}\text{Ni}_{0.33})\text{O}_2$ powder was synthesized from $\text{LiOH} \cdot \text{H}_2\text{O}$ (Aldrich) and $\text{Co}_{0.33}\text{Mn}_{0.33}\text{Ni}_{0.33}(\text{OH})_x$ ($x \sim 2$) precursors. The $\text{Co}_{0.33}\text{Mn}_{0.33}\text{Ni}_{0.33}(\text{OH})_x$ precursor was prepared by co-precipitation of the required amounts of the nitrate salts, $\text{M}(\text{NO}_3)_2$ (M = Co, Mn, Ni; Aldrich). After intimate grinding, the powdered mixture was pressed into a pellet and fired according to a two-step procedure. First, a low-temperature calcination step was performed at 480 °C in air for 5 h. Thereafter, a sintering step was carried out at 900 °C for 3 h followed by rapid quenching to room temperature. After grinding the pellet into a fine powder, the $\text{Li}(\text{Co}_{0.33}\text{Mn}_{0.33}\text{Ni}_{0.33})\text{O}_2$ electrodes were pre-conditioned prior to cell assembly by subjecting them to ammonia gas at 250 and 350 °C for 20 h in a tubular furnace.

Composite $0.3\text{Li}_2\text{MnO}_3 \cdot 0.7\text{LiMn}_{0.5}\text{Ni}_{0.5}\text{O}_2$ electrode powders were prepared directly from $\text{Ni}_{1-x}\text{Mn}_x(\text{OH})_2$ and $\text{LiOH} \cdot \text{H}_2\text{O}$ precursors using the required Li:Mn:Ni ratio. The $\text{Ni}_{1-x}\text{Mn}_x(\text{OH})_2$ precursor was prepared by precipitation from a basic solution containing $\text{Ni}(\text{NO}_3)_2$ and $\text{Mn}(\text{NO}_3)_2$ (pH $\sim$ 11). The reagents were intimately mixed in an acetone slurry, dried overnight and subsequently fired in air, first at 480 °C for 12 h and then at 900 °C for 5 h. Thereafter, the $0.3\text{Li}_2\text{MnO}_3 \cdot 0.7\text{LiMn}_{0.5}\text{Ni}_{0.5}\text{O}_2$ product was quenched to room temperature, also in air and ground into a fine powder. The $0.3\text{Li}_2\text{MnO}_3 \cdot 0.7\text{LiMn}_{0.5}\text{Ni}_{0.5}\text{O}_2$ electrode powder was pre-conditioned prior to cell assembly in two ways: (1) subjecting the powder to flowing ammonia gas at 200 °C for 20 h and (2) washing the powder in 0.1 M HNO_3 (pH $\sim$ 1.8) for 5 h before subjecting it to flowing ammonia gas at 200 °C for 20 h. The lithium, manganese and nickel contents in the parent and acid-treated compounds were determined by inductively coupled plasma-optical emission spectrometry (ICP-OES) on a Perkin-Elmer Optima 3300 Dual-View system.

2.2. Structural characterization

Powder X-ray diffraction patterns of the $\text{Li}(\text{Co}_{0.33}\text{Mn}_{0.33}\text{Ni}_{0.33})\text{O}_2$ and composite $0.3\text{Li}_2\text{MnO}_3 \cdot 0.7\text{LiMn}_{0.5}\text{Ni}_{0.5}\text{O}_2$ electrode powders were recorded before and after the pre-conditioning steps on a Siemens D-5000 diffractometer with Cu Kα radiation. Lattice parameters were determined by iterative Rietveld refinements of the diffraction profiles using the GSAS program [20].

2.3. Electrochemical measurements

For the electrochemical studies, cells were constructed as follows. The positive electrodes for the cells consisted of 84% (by mass) of the active $\text{Li}(\text{Co}_{0.33}\text{Mn}_{0.33}\text{Ni}_{0.33})\text{O}_2$ or composite $0.3\text{Li}_2\text{MnO}_3 \cdot 0.7\text{LiMn}_{0.5}\text{Ni}_{0.5}\text{O}_2$ material, intimately mixed with 8% polyvinylidene difluoride (PVDF) polymer binder (Kynar, Elf-Atochem), 4% acetylene black (Cabot) and 4% graphite (SFG-6, Timcal). Electrode laminates were cast from slurries of the electrode powders in 1-methyl-2-pyrrolidinone (NMP, Aldrich) onto Al current collector foils using a doctor blade. The laminates were subsequently dried, first at 75 °C for 10 h and, thereafter, under vacuum at 70 °C for 12 h. The electrolyte was 1 M LiPF_6 in ethylene carbonate (EC):di-ethyl carbonate (DEC) (1:1 mixture). Electrodes were evaluated at room temperature and at 50 °C in coin-type cells (size CR2032, Hohsen) with a lithium-foil counter electrode (FMC Corporation) and a polypropylene separator (Celgard 2400). Cells were assembled inside a He-filled glove box (<5 ppm H_2O and O_2) and cycled on a Maccor Series 2000 tester under galvanostatic mode with a constant current density of 0.1 mA cm^{-2} between either 4.45 and 2.5 V or between 4.6 and 2.0 V. Cyclic voltammograms of $\text{Li}(\text{Co}_{0.33}\text{Mn}_{0.33}\text{Ni}_{0.33})\text{O}_2$- and NH_3-treated $\text{Li}(\text{Co}_{0.33}\text{Mn}_{0.33}\text{Ni}_{0.33})\text{O}_2$ electrodes were recorded at room temperature between 4.6 and 2.0 V at a sweep rate of 0.02 mV s^{-1} with a Solartron 1480 potentiostat.
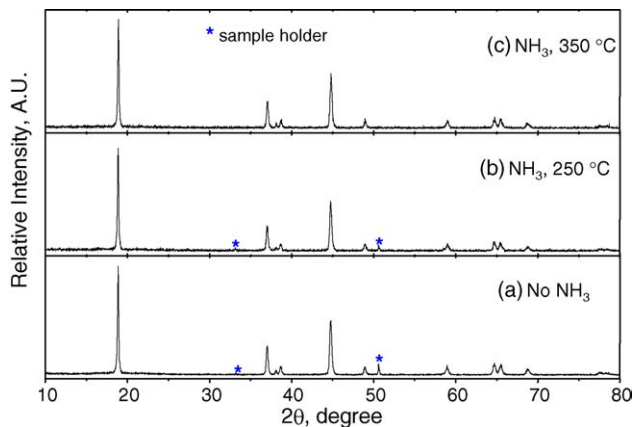
Fig. 1. Powder X-ray diffraction patterns of $Li(Co_{0.33}Mn_{0.33}Ni_{0.33})O_2$: (a) untreated; (b) after treatment with NH_3 at 250 °C; (c) after treatment with NH_3 at 350 °C.

3. Results and discussion

3.1. $Li(Co_{0.33}Mn_{0.33}Ni_{0.33})O_2$ electrodes

The X-ray diffraction patterns of a parent $Li(Co_{0.33}Mn_{0.33}Ni_{0.33})O_2$ electrode powder and products after treatment with NH_3 at 250 and 350 °C are shown in Fig. 1a–c, respectively. There are no major differences in the X-ray patterns, nor were there any significant changes to the refined lattice parameters of the parent compound, which were consistent with those reported by Ohzuku and co-worker [21], indicating that ammonia treatment had not affected the bulk structure of $Li(Co_{0.33}Mn_{0.33}Ni_{0.33})O_2$.

NH_3-treated $Li(Co_{0.33}Mn_{0.33}Ni_{0.33})O_2$ electrodes showed superior electrochemical properties to unconditioned electrodes. Electrochemical data for electrodes pre-conditioned at 250 °C were marginally superior to those treated at 350 °C; only the 250 °C data set were, therefore, used to compare the electrochemical properties of NH_3-treated electrodes with unconditioned electrodes. Typical voltage profiles, recorded at room temperature and at 50 °C and capacity versus cycle number plots of four independent lithium cells with untreated and NH_3-treated electrodes are shown in (Fig. 2a–d) to highlight the differences in their electrochemical behavior. Despite the fact that our capacities for $LiMn_{0.33}Ni_{0.33}Co_{0.33}O_2$ are slightly lower than those reported by others [21], the data from duplicate cells showed consistently that the capacity delivered by NH_3-treated $LiMn_{0.33}Ni_{0.33}Co_{0.33}O_2$ electrodes was superior to that delivered by the untreated $LiMn_{0.33}Ni_{0.33}Co_{0.33}O_2$ electrodes. For example, in Fig. 2a, the discharge capacity delivered at room temperature on the 15th cycle by an NH_3-treated $LiMn_{0.33}Ni_{0.33}Co_{0.33}O_2$ electrode *at a C*/18 rate (0.1 mA cm^{-2}) was 188 mAh g^{-1} in

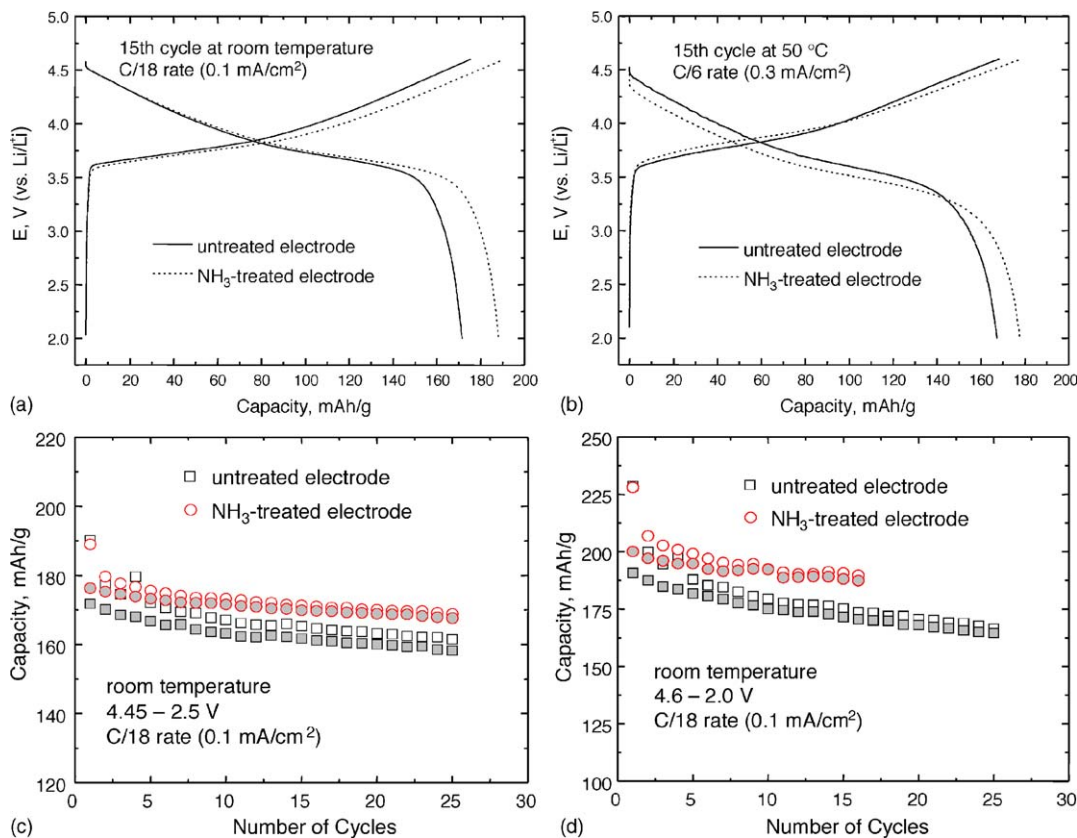Fig. 2. Electrochemical data of $Li/Li(Co_{0.33}Mn_{0.33}Ni_{0.33})O_2$ cells. Voltage profiles of lithium cells with untreated and NH_3-treated electrodes at: (a) room temperature and (b) 50 °C. Capacity vs. cycle number plots for cells operated at room temperature: (c) 4.45–2.5 V; (d) 4.6–2.0 V.

contrast to 171 mAh g^{-1} delivered by an untreated electrode at the same rate. At 50 °C and at three-times the rate (*C*/6, 0.3 mA cm^{-2}), the corresponding capacities were 177 and 167 mAh g^{-1}, respectively (Fig. 2b).

Fig. 2c and d compares the room temperature cycling stabilities of unconditioned and NH$_3$-treated LiMn$_{0.33}$Ni$_{0.33}$Co$_{0.33}$O$_2$ electrodes when cells were cycled between 4.45 and 2.5 V and between 4.6 and 2.0 V, respectively. The data confirm that NH$_3$-treatment increases electrode capacity; the data also demonstrate that NH$_3$-treatment improves the coulombic efficiency of the charge/discharge cycles. For example, in Fig. 2c and d, the coulombic efficiency of cells with untreated electrodes at the 15th cycle is 97.9 and 96.1%, whereas for cells with NH$_3$-treated electrodes the efficiency is increased to 99.1 and 97.2%, respectively. However, NH$_3$-treatment does not have a major effect on improving the low coulombic efficiency of the initial charge/discharge cycle of these cells; for these cells, the coulombic efficiency of the first cycle increases less significantly on NH$_3$-treatment from 90.5 to 93.1% (Fig. 2c) and from 83.2 to 86.8% (Fig. 2d). Although the precise reasons for the improvements in capacity and coulombic efficiency are not yet fully understood, we believe that mild reduction of the LiMn$_{0.33}$Ni$_{0.33}$Co$_{0.33}$O$_2$ electrode surface may contribute to stabilizing the electrode/electrolyte interface by lowering the oxidation potential of the electrode at high cell voltages (>4.2 V).

The differences between the first and second (oxidation) reactions that occur during charge at the surface of LiMn$_{0.33}$Ni$_{0.33}$Co$_{0.33}$O$_2$ and NH$_3$-treated LiMn$_{0.33}$Ni$_{0.33}$Co$_{0.33}$O$_2$ electrodes were monitored by cyclic voltammetry (Fig. 3a–c). The cyclic voltammogram of an untreated LiMn$_{0.33}$Ni$_{0.33}$Co$_{0.33}$O$_2$ electrode is shown in (Fig. 3a). On the initial sweep, the first oxidative process (1a) is attributed to lithium extraction from LiMn$_{0.33}$Ni$_{0.33}$Co$_{0.33}$O$_2$ and the concomitant oxidation of the transition metal ions, predominantly nickel; this process is reversible (1c). A second, irreversible process that occurs above 4.25 V (1b) is attributed to electrolyte oxidation. On the second oxidative sweep, lithium extraction (2a) occurs at a lower potential compared to process (1a) indicating that the electrode surface had been reduced during the initial electrolyte oxidation reaction (1b). The onset of the second electrolyte oxidation reaction (2b) is shifted to higher potential, which suppresses the magnitude of the reaction at 4.5–4.6 V. We speculate that the suppression of electrolyte oxidation at these high potentials may be a result of a protective layer that forms at the electrode surface during process (1b). The same effects were observed for LiMn$_{0.33}$Ni$_{0.33}$Co$_{0.33}$O$_2$ electrodes treated with NH$_3$ at 250 °C (Fig. 3b) and at 350 °C (Fig. 3c). However, in these instances, peaks (2a and 1a) become more closely aligned, consistent with our belief that the electrode surfaces are reduced by NH$_3$, slightly more so at 350 than 250 °C. Our overall conclusion is that although NH$_3$-treatment appears
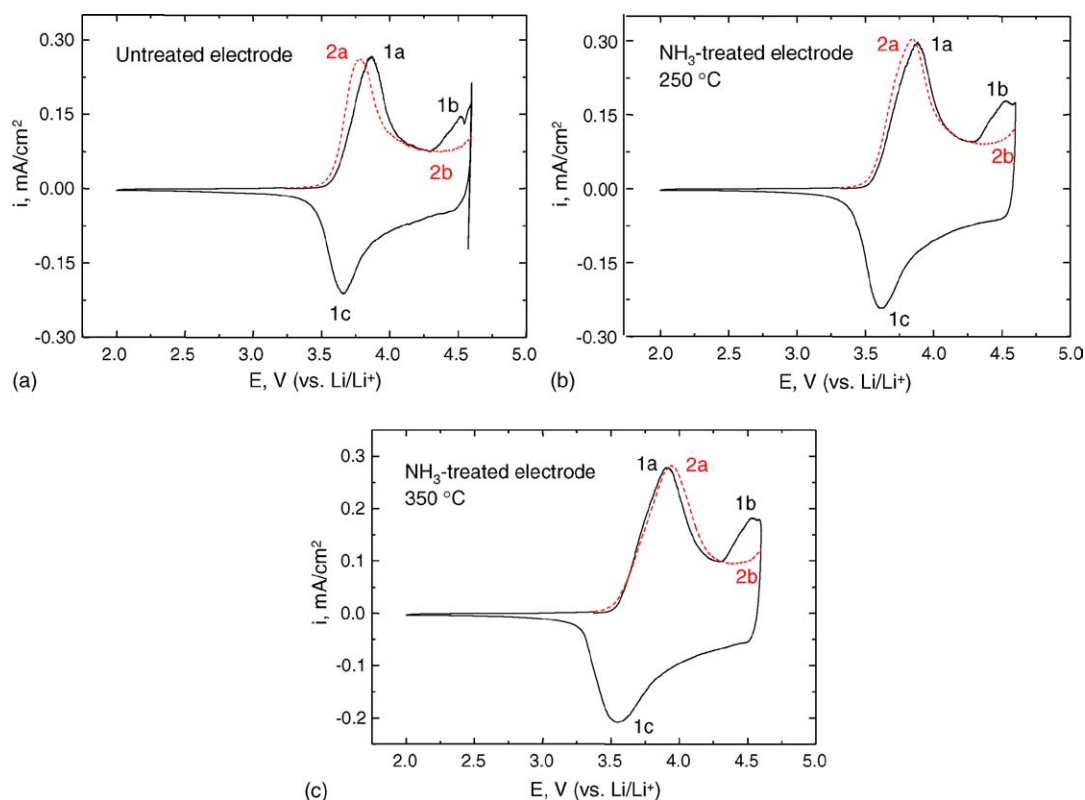

Fig. 3. Cyclic voltammograms of Li(Co$_{0.33}$Mn$_{0.33}$Ni$_{0.33}$)O$_2$ electrodes: (a) untreated; (b) after treatment with NH$_3$ at 250 °C; (c) after treatment with NH$_3$ at 350 °C.
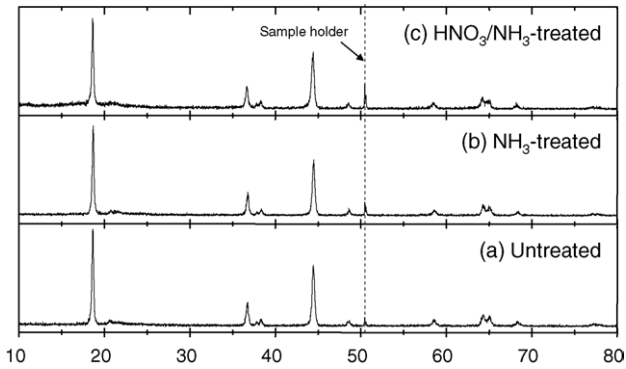
Fig. 4. Powder X-ray diffraction patterns of $0.3Li_2MnO_3 \cdot 0.7LiMn_{0.5}Ni_{0.5}O_2$: (a) untreated; (b) after treatment with NH_3 at 200 °C; (c) after treatment with 0.1 M HNO_3 and thereafter NH_3 at 200 °C.

Table 1
Lattice parameters of $0.3Li_2MnO_3 \cdot 0.7LiMn_{0.5}Ni_{0.5}O_2$ electrodes

Electrode	a (Å)	c (Å)
Untreated $0.3Li_2MnO_3 \cdot 0.7LiMn_{0.5}Ni_{0.5}O_2$	2.8655 (3)	14.254 (3)
NH_3-treated $0.3Li_2MnO_3 \cdot 0.7LiMn_{0.5}Ni_{0.5}O_2$	2.8666 (3)	14.259 (3)
HNO_3/NH_3-treated $0.3Li_2MnO_3 \cdot 0.7LiMn_{0.5}Ni_{0.5}O_2$	2.8711 (3)	14.271 (4)

to reduce the $LiMn_{0.33}Ni_{0.33}Co_{0.33}O_2$ electrode surface to some extent, it does not contribute significantly to the formation of the protective layer because oxidation of the electrolyte was not suppressed during the initial charge to 4.6 V.

3.2. Composite $0.3Li_2MnO_3 \cdot 0.7LiMn_{0.5}Ni_{0.5}O_2$ electrodes

Powder X-ray diffraction patterns of a $0.3Li_2MnO_3 \cdot 0.7LiMn_{0.5}Ni_{0.5}O_2$ electrode showed that the structure remained essentially unchanged after NH_3- and HNO_3 treatment (Fig. 4a–c). Despite the structural complexity of these composite electrodes [11], it was possible to determine the approximate lattice parameters of the parent $0.3Li_2MnO_3 \cdot 0.7LiMn_{0.5}Ni_{0.5}O_2$ compound and NH_3- and HNO_3-treated samples by profile refinement of their X-ray patterns. Trigonal symmetry (R-3m), characteristic of the layered $LiCoO_2$ structure, was used for these refinements. Table 1 shows that NH_3-treatment did not significantly affect the lattice parameters of $0.3Li_2MnO_3 \cdot 0.7LiMn_{0.5}Ni_{0.5}O_2$. By contrast, acid-treatment caused a small expansion of the

a and c lattice parameters, indicating that some lithium had been removed from the structure. Chemical analyses by ICP-OES showed that approximately 30% of the lithium was removed from $0.3Li_2MnO_3 \cdot 0.7LiMn_{0.5}Ni_{0.5}O_2$ by the reaction with acid, whereas the relative amounts of manganese and nickel were unaltered by this process.

The voltage profiles of the first charge/discharge cycle of lithium cells containing: (1) an untreated $0.3Li_2MnO_3 \cdot 0.7LiMn_{0.5}Ni_{0.5}O_2$ electrode; (2) an NH_3-treated electrode; (3) an HNO_3/NH_3-treated electrode are shown in Fig. 5a–c, respectively. Corresponding capacity versus cycle number plots for the cells are shown in Fig. 6a–c. The coulombic efficiency of the initial cycle of each of the cells, as determined from the electrode capacity measured during charge and discharge are summarized in Table 2. The data show that $0.3Li_2MnO_3 \cdot 0.7LiMn_{0.5}Ni_{0.5}O_2$ electrodes that had been treated with NH_3 did not affect the efficiency of the first charge/discharge cycle. By contrast, electrodes that had been subjected to mild acid-treatment (0.1 M HNO_3 for 5 h) showed a surprisingly large improvement in first-cycle efficiency: 78–95%. This finding has been confirmed in duplicate cells. The reasons for the improvement have not yet been determined, nor has the extent of possible H^+–Li^+ exchange. Despite the preliminary nature of our work, it is tempting to speculate that the improved efficiency of the first charge/discharge cycle may be coupled to the amount of 'MnO_2' generated either by Li_2O extraction from the Li_2MnO_3 component of the composite structure by acid-treatment (akin to the process that occurs electrochemically during the initial charge of Li/$0.3Li_2MnO_3 \cdot 0.7LiMn_{0.5}Ni_{0.5}O_2$ cells) because a MnO_2 component, particularly at the electrode surface might be more resistant to electrolyte oxidation at 4.6 V than the parent $0.3Li_2MnO_3 \cdot 0.7LiMn_{0.5}Ni_{0.5}O_2$ electrode. The observation that the upper voltage limit (4.6 V) is reached more rapidly when an acid-treated electrode is used lends credence to this hypothesis. Moreover, the inflection point at approximately 3.25 V in Fig. 5a and b, which has been attributed to the reduction of the MnO_2 component ($Mn^{4+/3+}$ couple) in electrochemically charged $0.3Li_2MnO_3 \cdot 0.7LiMn_{0.5}Ni_{0.5}O_2$ electrodes [11], is significantly suppressed in Fig. 5c, suggesting that there is less MnO_2 in the acid-treated $0.3Li_2MnO_3 \cdot 0.7LiMn_{0.5}Ni_{0.5}O_2$ electrode structure. The remarkable cycling stability of these composite electrodes, when cycled between 4.6 and 2.0 V versus Li^0, confirms the reports of others [3,13]; they yield stable capacities in excess of 200 mAh g^{-1} (Fig. 6a–c).

Table 2
Initial charge/discharge capacities and coulombic efficiency (%) of lithium cells with $0.3Li_2MnO_3 \cdot 0.7LiMn_{0.5}Ni_{0.5}O_2$ electrodes (4.6–2.0 V)

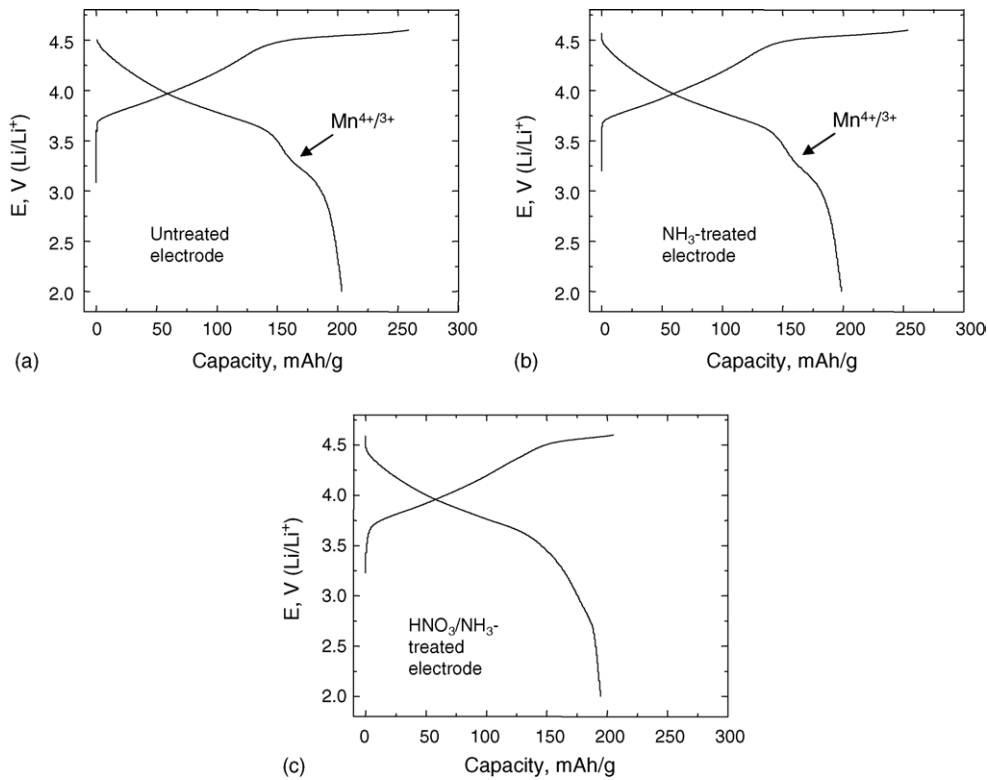| Electrode	Initial charge capacity (mAh g^{-1})	Initial discharge capacity (mAh g^{-1})	Coulombic efficiency (%)
$0.3Li_2MnO_3 \cdot 0.7LiMn_{0.5}Ni_{0.5}O_2$	259	203	78
NH_3-treated $0.3Li_2MnO_3 \cdot 0.7LiMn_{0.5}Ni_{0.5}O_2$	254	199	78
HNO_3/NH_3-treated $0.3Li_2MnO_3 \cdot 0.7LiMn_{0.5}Ni_{0.5}O_2$	205	195	95

Fig. 5. Voltage profiles of lithium cells with untreated and pre-conditioned $0.3Li_2MnO_3 \cdot 0.7LiMn_{0.5}Ni_{0.5}O_2$ electrodes: (a) untreated; (b) after treatment with NH_3 at 200 °C; (c) after treatment with 0.1 M HNO_3 and thereafter NH_3 at 200 °C.
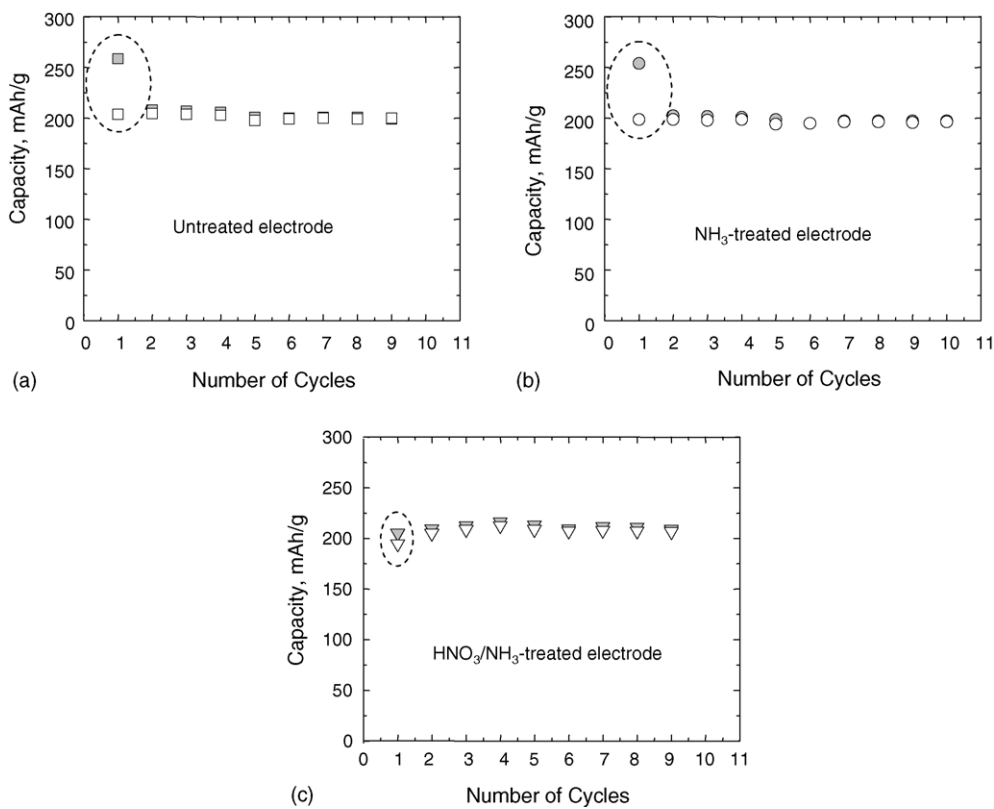

Fig. 6. Capacity vs. cycle number plots of lithium cells with untreated and pre-conditioned $0.3Li_2MnO_3 \cdot 0.7LiMn_{0.5}Ni_{0.5}O_2$ electrodes: (a) untreated; (b) after treatment with NH_3 at 200 °C; (c) after treatment with 0.1 M HNO_3 and thereafter NH_3 at 200 °C.

4. Conclusions

Pre-conditioning layered lithium-transition metal oxide electrodes by mild NH_3-treatment or by acid-treatment can improve their electrochemical properties when charged to high potentials (4.6 V). NH_3-treatment of $Li(Co_{0.33}Mn_{0.33}Ni_{0.33})O_2$, which reduces the electrode surface, has the effect of increasing the delivered capacity, whereas acid-treatment of composite electrode structures with an Li_2MnO_3 component, such as $0.3Li_2MnO_3 \cdot 0.7LiMn_{0.5}Ni_{0.5}O_2$, significantly reduces the first-cycle irreversible capacity loss, consistent with the removal of some Li_2O from the structure. These data suggest, in particular, that these processing routes may be of use for controlling the composition and performance of high-capacity, Mn-rich composite electrodes ($>200\,mAh\,g^{-1}$) in which the manganese ions play an important role in stabilizing the electrode at high potentials.

Acknowledgments

References

[1] M.E. Spahr, P. Novak, B. Schnyder, O. Haas, R. Nesper, J. Electrochem. Soc. 14 (1998) 1113.
[2] T. Ohzuku, Y. Makimura, Chem. Lett. (2001) 744.
[3] Z. Lu, D.D. MacNeil, J.R. Dahn, Electrochem. Solid State Lett. 4 (2001) 191.
[4] C.S. Johnson, J.-S. Kim, A.J. Kropf, A.J. Kahaian, J.T. Vaughey, M.M. Thackeray, Chem. Mater. 15 (2003) 2313.
[5] T. Ohzuku, Y. Makimura, Chem. Lett. (2001) 642.
[6] Z. Lu, D.D. MacNeil, J.R. Dahn, Electrochem. Solid State Lett. 4 (2001) 200.
[7] I. Belharouak, Y.-K. Sun, J. Liu, K. Amine, J. Power Sources 122–123 (2003) 247.
[8] J.K. Ngala, N.A. Chernova, M. Ma, M. Mamak, P.Y. Zavalij, M.S. Whittingham, J. Mater. Chem. 14 (2004) 214.
[9] M.H. Rossouw, M.M. Thackeray, Mater. Res. Bull. 26 (1991) 463.
[10] C.S. Johnson, M.M. Thackeray, in: A.R., Landgrebe, R.J., Klingler (Eds.), Interfaces, Phenomena, and Nanostructures in Lithium Batteries, The Electrochem. Soc. Inc. Proc. PV 2000–36 (2001) 47.
[11] J.-S. Kim, C.S. Johnson, J.T. Vaughey, M.M. Thackeray, S.A. Hackney, W. Yoon, C.P. Grey, Chem. Mater. 16 (2004) 1996.
[12] K. Numata, S. Yamanaka, Solid State Ionics 118 (1999) 117.
[13] Z. Lu, J.R. Dahn, J. Electrochem. Soc. 149 (2002) 815.
[14] M. Balasubramanian, J. McBreen, I.J. Davidson, P.S. Whitfield, I. Kargina, J. Electrochem. Soc. 149 (2002) 176.
[15] B. Ammundsen, J. Paulsen, I. Davidson, R.-S. Liu, C.-H. Shen, J.-M. Chen, L.-Y. Yang, J.-F. Lee, J. Electrochem. Soc. 149 (2002) 431.
[16] M.H. Rossouw, D.C. Liles, M.M. Thackeray, J. Solid State Chem. 104 (1993) 464.
[17] W. Tang, H. Kanoh, X. Yang, K. Ooi, Chem. Mater. 12 (2000) 3271.
[18] Y. Paik, C.P. Grey, C.S. Johnson, J.-S. Kim, M.M. Thackeray, Chem. Mater. 14 (2002) 5109.
[19] M.N. Richard, E.W. Fuller, J.R. Dahn, Solid State Ionics 73 (1994) 81.
[20] A.C. Larson, R.B. Von Dreele, GSAS, General Structure Analysis System, Report No. LA-UR-86-748, Los Alamos National Laboratory, Los Alamos, NM, 1990.
[21] N. Yabuuchi, T. Ohzuku, J. Power Sources 119–121 (2003) 171.